Tissue Inhibitor of Metalloproteinase-1 Deficiency Amplifies Acute Lung Injury in Bleomycin-Exposed Mice

Kyoung-Hee Kim[*], Kristin Burkhart[*], Peter Chen[*,‡], Charles W. Frevert[‡], Julie Randolph-Habecker[†], Robert C. Hackman [†,§], Paul D. Soloway [‖], David K. Madtes [*,‡]

Sections of Pulmonary and Critical Care Medicine[*] and Pathology[†], Fred Hutchinson Cancer Research Center; Departments of Medicine[‡] and Pathology[§], University of Washington School of Medicine, Seattle, Washington and Division of Nutritional Sciences[‖], Cornell University, Ithaca, New York.

Address correspondence to: David K. Madtes, M.D.

Fred Hutchinson Cancer Research Center

1100 Fairview Avenue N, D3-190

P.O. Box 19024

Seattle, WA. 98109-1024

Telephone: (206) 667-4589 Facsimile: (206) 667-5765

E-mail address: dmadtes@fhcrc.org

Online Supplement

Am J Respir Cell Mol Biol Vol 33, pp. 271–279, 2005.

Materials and Methods

Immunohistochemistry. Antigen retrieval was performed on 5-μm sections of mouse lung tissue using citrate buffer pH 6.0 at 85-90^{o}C for 20 min. Endogenous avidin/biotin was blocked using an Avidin/Biotin blocking kit (Vector Laboratories, Burlingame, CA) and endogenous peroxidase activity was blocked by incubation of the sections in 3% hydrogen peroxide (Medi-pak, McKesson Corp, Richmond, VA). The sections were protein blocked by using 15% normal donkey serum plus 5% normal mouse serum (Jackson ImmunoResearch Laboratories, West Grove, PA) at RT for a period of 10 min. Affinity purified goat polyclonal antibody to mouse recombinant TIMP-1 (R & D Systems) was then applied to the tissue at a 1:400 dilution for 30 min at RT. The secondary reagent, biotinylated donkey anti-goat antibody (Jackson ImmunoResearch), was applied at a 1:200 dilution at RT for 30 min. Secondary antibody was detected using an RTU Vectastain kit (Vector Laboratories,) for 30 min at RT following the manufacturer's protocol. Bound antibody was visualized with the Envision DAB kit (Dako Cytomation, Dako Corp, Carpinteria, CA) and the sections were counter stained with hematoxylin. Digital photomicrographs were produced with a Nikon E600 photomicroscope and MetaMorph 4.6 software. The digitized images were processed by means of Adobe Photoshop for Windows 7.0 software (Adobe Systems, Inc. Mountainview, CA) using identical parameters for all images. As a negative control, serial sections were stained with irrelevant goat IgG.

PMN Migration through Matrigel. Murine bone marrow-derived neutrophils were isolated as previously described (E1), suspended at 1 x 10^{6}/ml in DMEM containing

0.1% BSA and placed in the upper compartment of the Matrigel Cell Invasion Chamber (Bectin Dickinson Labware, Bedford, MA). The lower compartment contained 5 nM recombinant KC in DMEM/0.1% BSA. The two compartments were separated by an 8 μm pore-size membrane coated with Matrigel. After 2 hr incubation at 37^{o}C in humidified 5% CO_2-air, the filter was stained with DiffQuik (Fisher Scientific) and mounted on a glass slide. The number of cells that migrated to the underside of the filter in four random high-power fields (x 400) was quantified for each of five filters for each genotype and condition. In addition, the total number of cells recovered from the lower compartment were counted on a hemocytometer in duplicate for each of five chambers for each genotype and condition. The neutrophils used in the migration assays were pooled from two TIMP-1 -/- or wild-type mice.

Neutrophil Chemotaxis Assay. Neutrophil chemotaxis was measured with a fluorescent chemotaxis assay as previously described using human neutrophils as the chemotactic targets (E2). Normal human neutrophils isolated by density gradient centrifugation (mono-poly resolving media, ICN Pharmaceuticals, Costa Mesa, CA) were labeled with calcein AM (Molecular Probes, Eugene, OR) and. resuspended at 3x 10^6 PMN/ml. The bottom wells of disposable 96 well chemotaxis chambers (ChemoTx; Neuro Probe Inc., Gaithersburg, MD) were filled with either 29 μl of BAL fluid diluted in PBS-human serum albumin (HSA) or with negative control (i.e. PBS supplemented with 1% HSA). To determine the total fluorescence of the labeled neutrophils, 25 μl of the cell suspension was placed directly in three bottom wells of the chemotaxis chamber. Polycarbonate filters with 8-μm pores were positioned on the loaded microplate and

calcein labeled neutrophils (25 μl) were placed directly onto the filter above each well. The chamber was incubated for 1 h at 37^{o}C in 5% CO_2-air, non-migrating cells on the top of the filter removed, and cells in the bottom chamber measured from the calcein fluorescence signal (excitation=485 nm, emission=530nm) using a multiwell fluorescence plate reader (Cytofluor II; PerSeptive Biosystems, Framingham, MA). The data for the chemotaxis assay were expressed as a percentage of the response to zymosan-activated normal human serum (ZAS) in the same assay.

References

E1. Nick JA, Young SK, Brown KK, Avdi NJ, Arndt PG, Suratt BT, Janes MS, Henson PM, Worthen GS. Role of p38 mitogen-activiated protein kinase in a murine model of pulmonary inflammation. *J Immunol.* 2000;164:2151-2159.

E2. Frevert CW, Wong VA, Goodman RB, Goodwin R, Martin TR. Rapid fluorescence-based measurement of neutrophil migration in vitro. *J Immunol Methods* 1998;213:41-52.

Figure Legends

Figure E1. Leukocyte concentrations in the BAL recovered from wild-type and TIMP-1 -/- mice after LPS administration.

Mean values (± SE) for total leukocytes, neutrophils, macrophages and lymphocytes in the BAL of TIMP-1 +/+ (white column) and TIMP-1 -/- (black column) mice recovered at 4 hours after LPS instillation (1 μg/gm BW). Six LPS injured mice were analyzed for each genotype.

Figure E2. Temporal changes in erythrocyte concentration in the BAL recovered from wild-type and TIMP-1 -/- mice after bleomycin administration.

Mean values (± SE) for erythrocyte concentration in the BAL of TIMP-1 +/+ (open squares) and TIMP-1 -/- (solid diamonds) mice after a single intratracheal dose of bleomycin. Six TIMP-1 +/+ and six TIMP-1 -/- mice were analyzed at each time point. * $p < 0.03$

Figure E3. Temporal changes in IgM concentration in the BAL recovered from wild-type and TIMP-1 -/- mice after bleomycin administration.

Mean values (± SE) for IgM concentration in the BAL of TIMP-1 +/+ (open squares) and TIMP-1 -/- (solid diamonds) mice before or after a single intratracheal dose of bleomycin. Six TIMP-1 +/+ and six TIMP-1 -/- mice were analyzed at each time point.

Figure E4. Temporal changes in body weight and survival of wild-type and TIMP-1-/- mice after bleomycin administration.

A. Mean values (± SE) for body weight of TIMP-1 +/+ (open squares) and TIMP-1 -/- (solid diamonds) mice after a single intratracheal dose of 0.007U/gm BW bleomycin. Six TIMP-1 +/+ and six TIMP-1 -/- mice were analyzed at each time point. * $p < 0.05$

B. Percent survival of TIMP-1 +/+ (open squares) and TIMP-1 -/- (solid diamonds) mice after a single intratracheal dose of 0.0035U/gm BW bleomycin. (n =14 mice per group, p=0.056 by log-rank test)

Figure E5. Gelatin zymography of BAL fluid collected from wild-type and TIMP-1 -/- mice at days 3 and 7 after intratracheal administration of bleomycin.

BAL fluid (40 μl) isolated from individual mice was electrophoresed on 10% polyacrylamide containing 1 mg/ml gelatin. Areas of gelatinolytic activity visualize as light bands after the gel is stained with Coomassie blue. Recombinant human MMP-9 (200 pg) serves as a positive control. Molecular weight markers are indicated at right. Gelatinolytic values were determined by densitometry and are expressed as relative absorbance of the sample lysis zone divided by the MMP-9 standard lysis zone and

indicated on the graph. The zymographic results shown are representative of duplicate experiments. Six TIMP-1 +/+ and six TIMP-1 -/- mice were analyzed at each time point. * $p < 0.04$

Figure E6. Temporal changes in KC, MIP-2, TNF-α and LIX concentrations in the BAL and lung homogenates of wild-type and TIMP-1 -/- mice after bleomycin administration.

Mean values (± SE) for KC concentration in BAL (A) and lung homogenate (B), for MIP-2 concentration in BAL (C) and lung homogenate (D), for TNF-α concentration in BAL (E) and lung homogenate (F) and for LIX concentration in BAL (G) and lung homogenate (H) of wild-type (open squares) and TIMP-1 -/- (solid diamonds) mice before or after a single intratracheal dose of bleomycin. Six wild-type and six TIMP-1 -/- mice were analyzed at each time point.

Figure E7. Temporal changes in lung hydroxyproline content of wild-type and TIMP-1 -/- mice after bleomycin administration.

Mean values (± SE) for hydroxyproline content of wild genotype (solid squares) and TIMP-1 -/- (solid diamonds) mice after a single intratracheal dose of bleomycin, and wild genotype (open squares) and TIMP-1 -/- (open diamonds) mice after a single dose of saline. Whole lung hydroxyproline values were determined by normalizing the hydroxyproline values obtained with the colorimetric assay of the minced lung aliquots to whole-lung wet weights. Six wild-type and six TIMP-1 -/- mice were analyzed for each condition at each time point. $p<0.01$ for comparison of wild-type bleomycin versus saline and for comparison TIMP-1-/- bleomycin versus saline at days 28, 45 and 60.

Figure E1

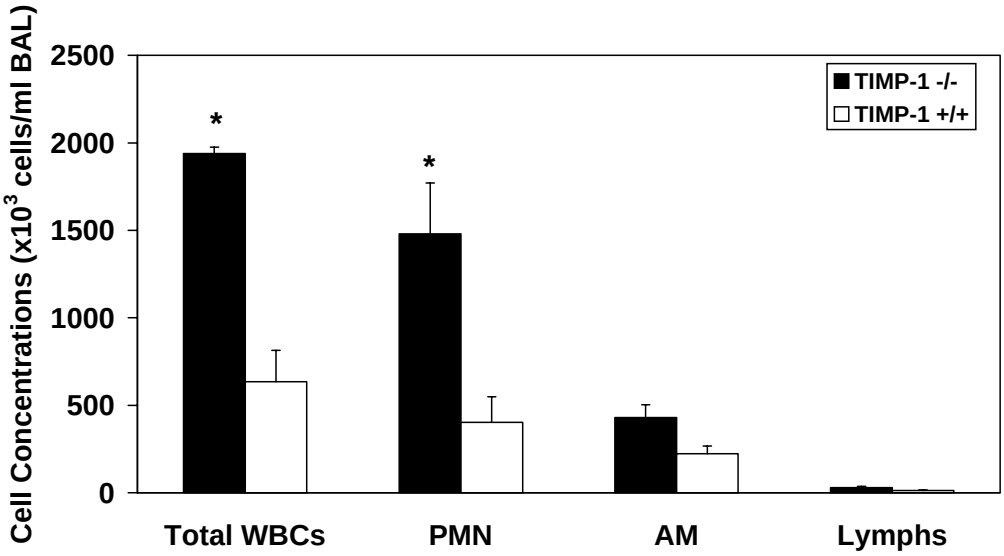

Figure E2

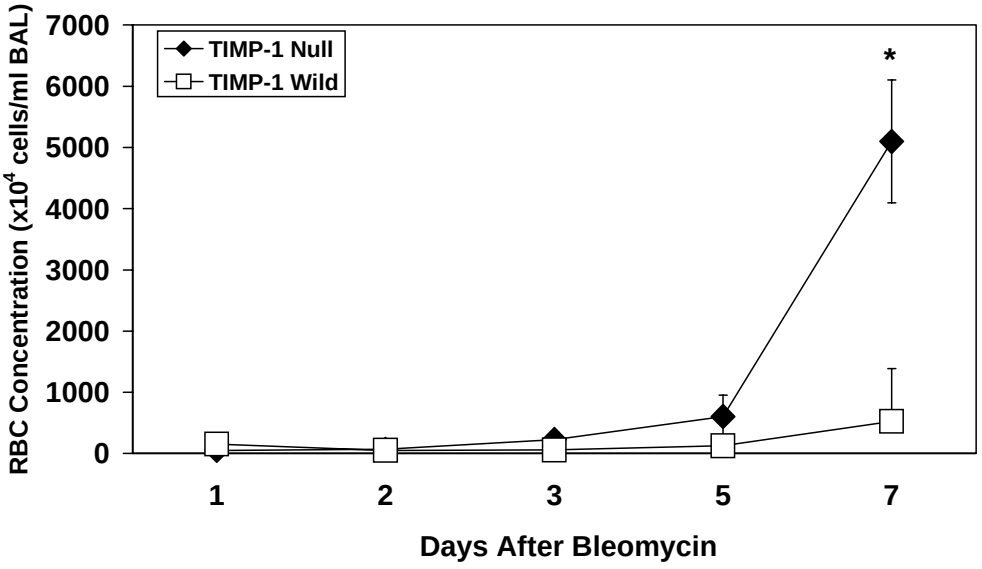

Figure E3

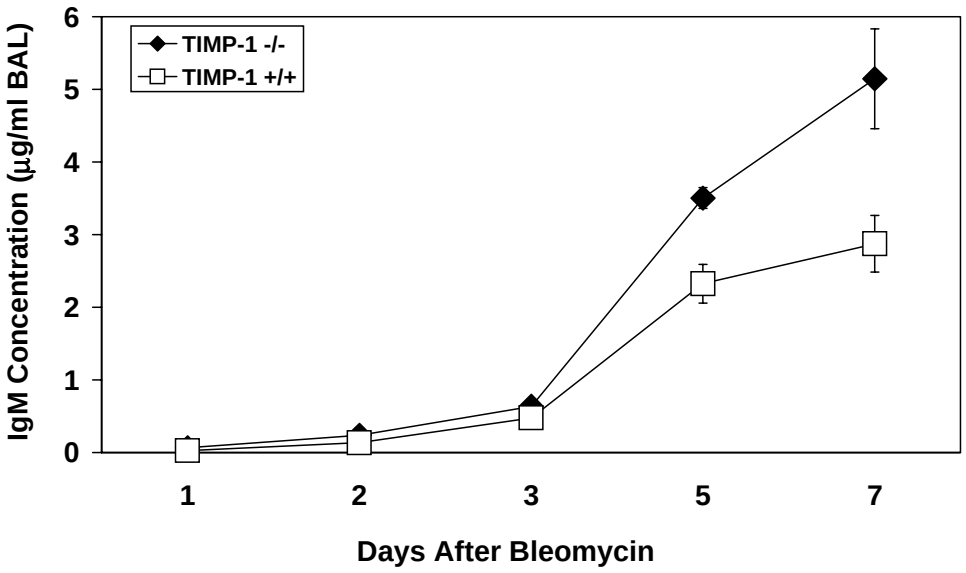
TIMP-1 -/-
TIMP-1 +/+
IgM Concentration (µg/ml BAL)
0
1
2
3
4
5
6
1
2
3
5
7
Days After Bleomycin

Figure E4
A.

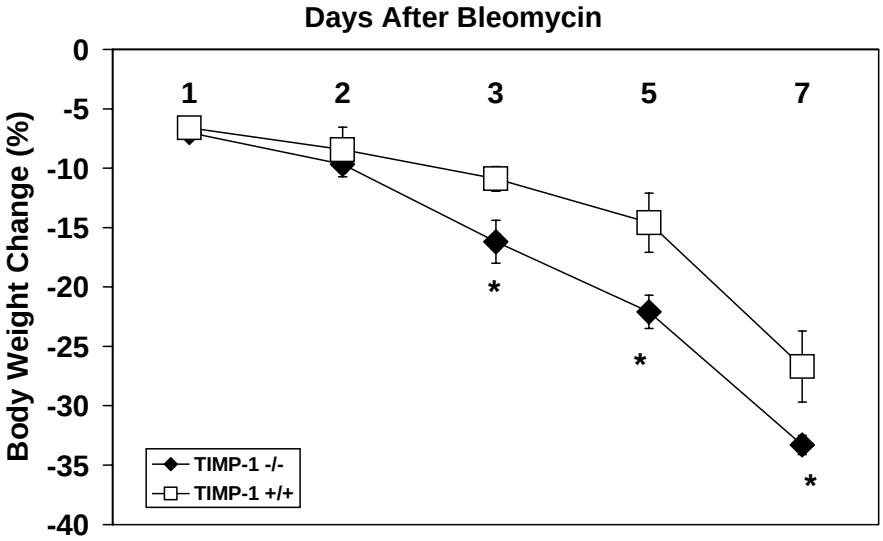
Days After Bleomycin
Body Weight Change (%)
0
-5
-10
-15
-20
-25
-30
-35
-40
1
2
3
5
7
*
*
*
TIMP-1 -/-
TIMP-1 +/+

B.

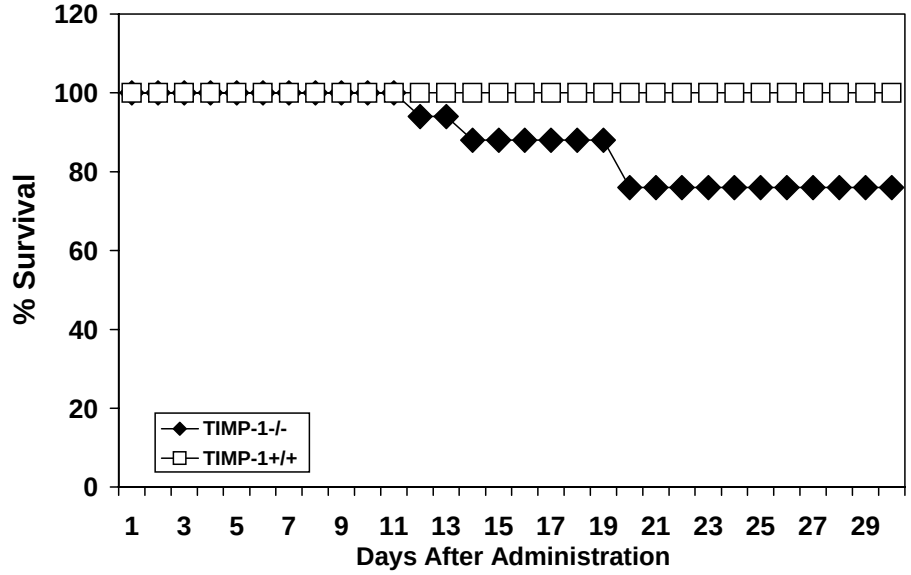
% Survival
120
100
80
60
40
20
0
1
3
5
7
9
11
13
15
17
19
21
23
25
27
29
Days After Administration
TIMP-1-/-
TIMP-1+/+

Figure E5

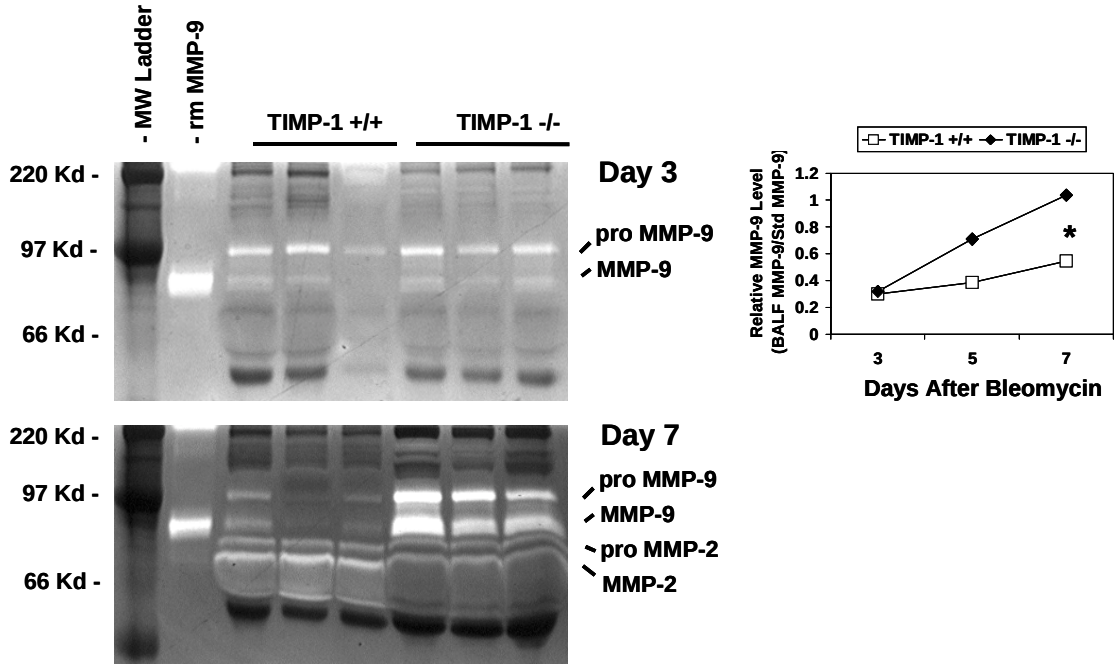

Figure E6

A. KC Concentration in BAL Fluid

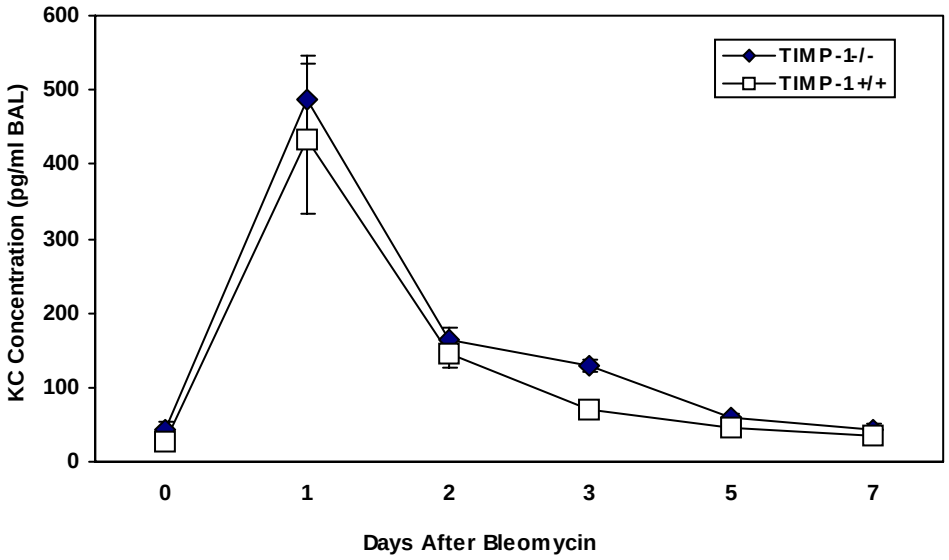

B. KC Concentration in Lung Homogenates

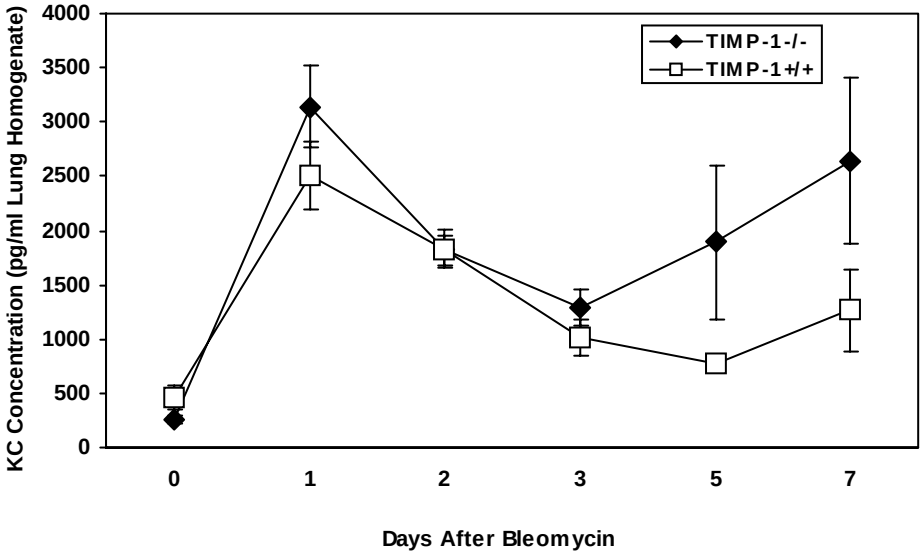

C. MIP-2 Concentrations in BAL Fluid

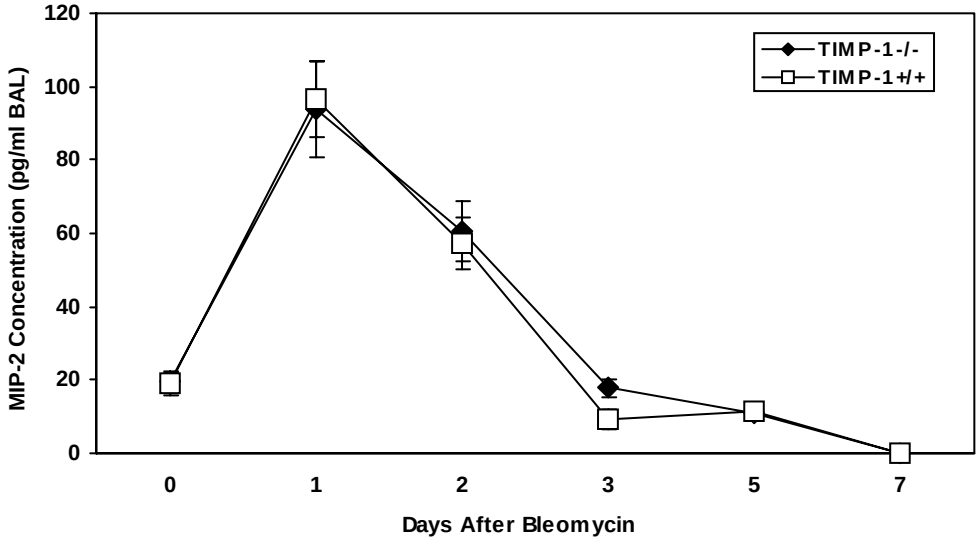

D. MIP-2 Concentrations in Lung Homogenates

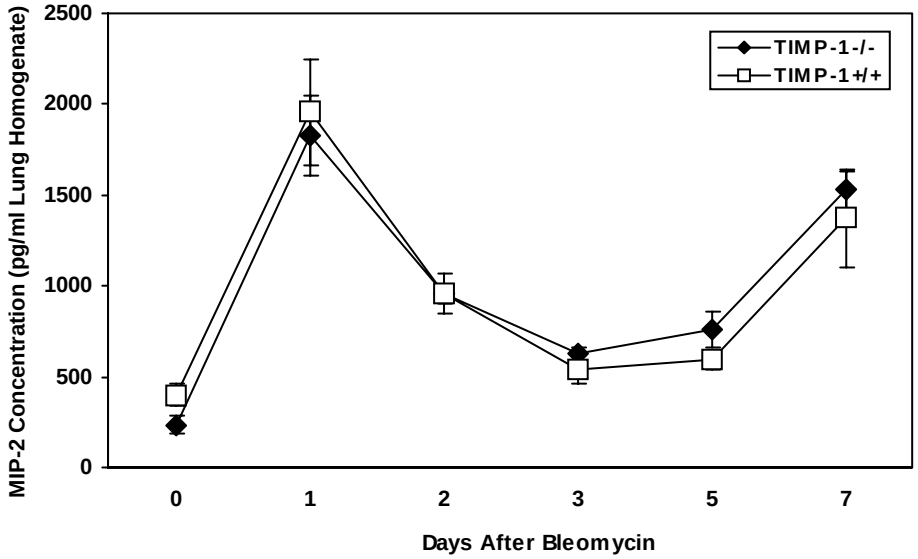

E. TNF-α Concentrations in BAL Fluid

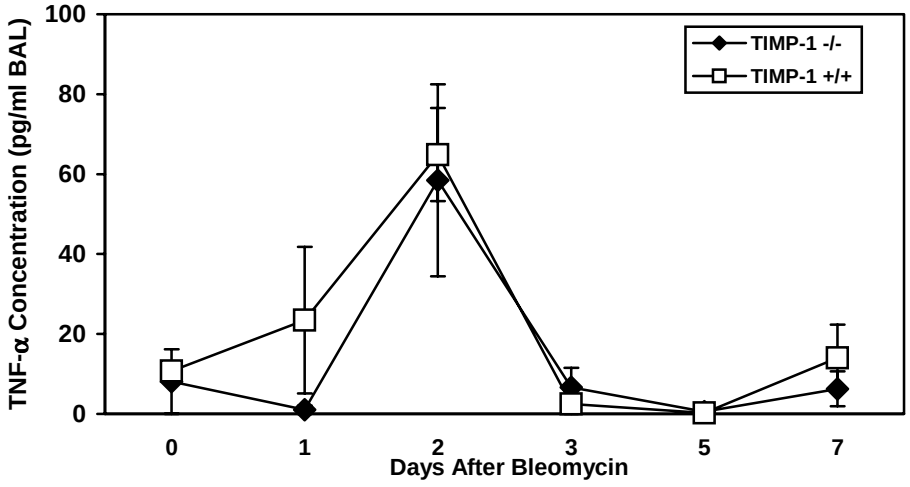

F. TNF-α Concentrations in Lung Homogenates

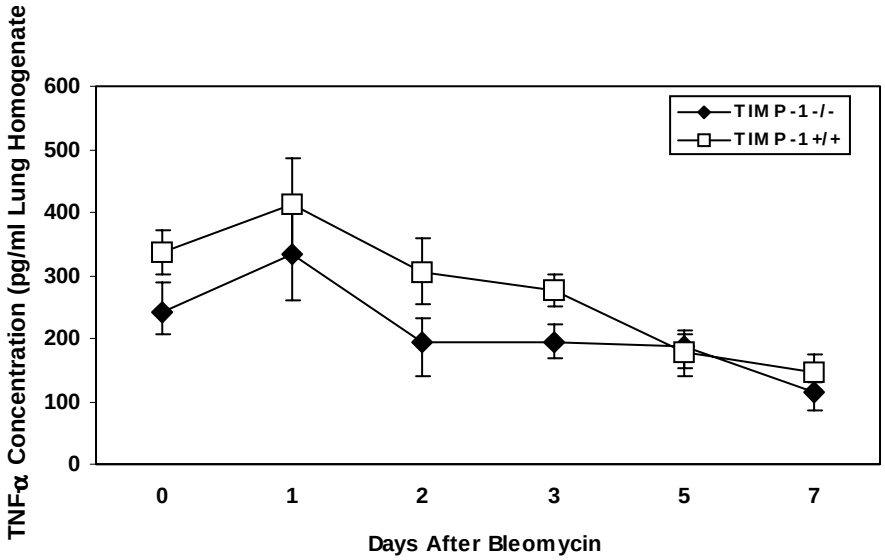

G. LIX Concentrations in BAL Fluid

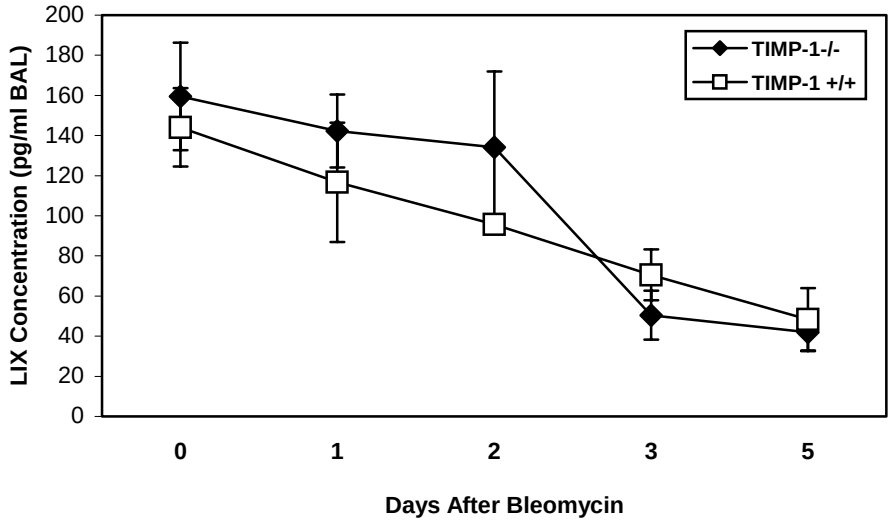

H. LIX Concentration in Lung Homogenates

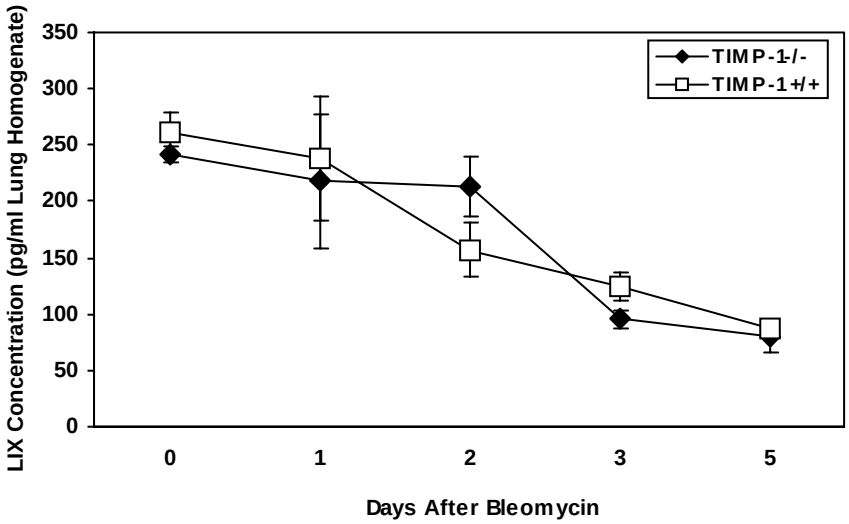

Figure E7